

Spin configurations of ABX_3 antiferromagnets in an external magnetic field

E. Rastelli and A. Tassi

Dipartimento di Fisica, Università di Parma, 43100 Parma, Italy

(Received 24 June 1994; revised manuscript received 22 August 1994)

Interesting compounds of the ABX_3 family can be modeled by antiferromagnetic chains arranged according to a triangular pattern, where each spin is coupled with six nearest neighbors via a weak interchain antiferromagnetic interaction. The behavior of this model in an external magnetic field perpendicular to the c axis has been studied when a sufficiently strong anisotropy forces the spins in the c plane in order to explain the low-temperature transition occurring in CsMnBr_3 . We find that interesting phenomena occur in the opposite limit of weak anisotropy. Indeed an *umbrella* configuration intervenes between the low-field *distorted-helix* configuration and the high-field *fan* configuration. We evaluate the elastic-neutron-scattering cross section and suggest CsVCl_3 , CsVBr_3 , and CsVI_3 as good candidates to test our theoretical prevision.

I. INTRODUCTION

The ABX_3 compounds, where A is an alkali element, B a magnetic ion, and X a halogen, have been extensively studied both experimentally¹ and theoretically.²

Indeed these compounds can be modeled by antiferromagnetic chains forming a hexagonal lattice so that the spins in the c plane are localized on a triangular lattice and are coupled by a weak antiferromagnetic interchain interaction. This is a well-known source of frustration inducing interesting reorientation phenomena when an external magnetic field is applied.² The ferromagnetic or antiferromagnetic nature of the strong intrachain interaction is crucial. The intrachain coupling is antiferromagnetic for the most part of the ABX_3 compounds, but it can be also ferromagnetic as in CsCuCl_3 .³ In the latter case the model behaves quite similarly to the triangular antiferromagnet,^{4,5} so that quantum and thermal fluctuations select the spin configuration out of a manifold of infinite configurations which are isoenergetic in the presence of an in-plane external magnetic field.^{6,7}

Magnetic resonance experiments in CsCuCl_3 (Ref. 8) are well understood on the basis of the spin configuration selected by quantum fluctuations accounted for in spin wave theory.^{3,9} Also the measurement of the magnetization as a function of the external magnetic field¹⁰ is explained by the spin wave theory.^{3,9} In particular, the plateau observed when the field is perpendicular to the c axis is explained as a first-order phase transition between a *distorted-helix* (H) configuration and a *fan* (F) phase.³ Also the jump of the magnetization observed when the magnetic field is parallel to the c axis¹⁰ is explained as a reorientation of the spins out of the c plane.¹¹

The antiferromagnetic intrachain coupling of the most part of the ABX_3 compounds provides good candidates to test experimentally interesting theoretical expectations. Indeed the interchain coupling is so weak that one expects the elementary excitation spectrum to keep track of the quantum scenario of the antiferromagnetic chain conjectured by Haldane.¹²

Another interesting topic is the behavior of the spin configuration in an external magnetic field since reorientation phenomena are expected. This scenario has been already investigated² when a sufficiently strong single-ion easy-plane anisotropy forces the spins into the c plane. In this case two second-order phase transitions are expected at increasing magnetic field; the former occurs between a six-sublattice H configuration and a four-sublattice F configuration similar to a spin-flop phase. The latter occurs between the F phase and the saturated (S) paramagnetic phase for a magnetic-field so high that cannot be obtained in laboratory.

Here we investigate the spin configurations in the limit of small easy-plane anisotropy. We find that below a triple point in the magnetic-field-anisotropy h - d plane, another spin configuration intervenes. Indeed an *umbrella* (U) phase with the axis parallel to the external magnetic field is stable over a substantial range of an intermediate magnetic field. The low-field spin configuration is still the H phase but a first-order phase transition to the U phase occurs. A second-order phase transition between the U and F phases is expected for a critical field very close to the saturation field. We find that the h - d plane is divided into four regions: H, U, F, and S corresponding to distorted helix, umbrella, fan, and saturated phases, respectively. The H-U boundary is first order whereas all other phase boundaries are second order. The H-U, U-F, and H-F boundary lines meet at a triple point above which the U phase disappears. The magnetic field at which the first-order H-U phase transition occurs is small (of the order of the weak interchain coupling) whereas the magnetic field at which the second-order U-F phase transition occurs is high (of the order of the strong intrachain coupling). So the U phase is a substantial feature of the model below the triple point.

The format of this paper is the following: In Sec. II the minimization of the classical energy for the hexagonal Heisenberg antiferromagnet with single-ion easy-plane anisotropy is performed. The main results are discussed for a selected choice of the Hamiltonian parameters. In Sec. III the elastic-neutron-scattering cross section is ob-

tained and discussed for the different spin configurations. Our theoretical results are applied to CsMnBr₃ and the expectation of a second-order H-F phase transition² is confirmed. We find a kink in the intensity of the (0,0,1) peak as function of the magnetic field in good agreement with the experimental result.¹³

When the easy-plane anisotropy is small enough and the U phase intervenes, the kink is replaced by a jump. We suggest elastic-neutron-scattering experiments in a magnetic field perpendicular to the *c* axis for CsVCl₃, CsVBr₃, and CsVI₃. Indeed such compounds, already investigated in zero magnetic field,^{14,15} should develop the U phase on the basis of our theoretical previsions keeping the Hamiltonian parameters suggested by inelastic-neutron-scattering experiment.¹⁵

We expect that our calculations are reliable although worked out in a classical approximation. Indeed crucial and interesting quantum effects on the elementary excitation spectrum related to the quasi-one-dimensional (quasi-1D) nature of the *ABX*₃ compounds certainly escape the classical approximation and linear spin wave approach,¹⁶ but the essential features of the ground state configurations should not be severely affected by quantum corrections owing to the high value of the spin and the 3D nature of the phases we consider. A summary and conclusions are contained in Sec. IV.

II. MINIMUM ENERGY SPIN CONFIGURATION

The Hamiltonian we consider reads

$$\mathcal{H} = 2J_{\parallel} \sum_n \mathbf{S}_n \cdot \mathbf{S}_{n+1} + 2J_{\perp} \sum_{\langle ij \rangle} \mathbf{S}_i \cdot \mathbf{S}_j + D \sum_i (S_i^z)^2 - g\mu_B \mathbf{H} \cdot \sum_i \mathbf{S}_i, \quad (2.1)$$

where $2J_{\parallel} > 0$ and $2J_{\perp} > 0$ are the antiferromagnetic exchange couplings between nearest neighbor pairs of spins along the *c* axis and in the *c* plane of a hexagonal lattice, respectively. $D > 0$ is the single-ion easy-plane anisotropy strength, \mathbf{H} is the external magnetic field, g is the Landé factor, and μ_B is the Bohr magneton.

The zero-field minimum energy configuration of the model Hamiltonian (2.1) is a six-sublattice configuration with antiferromagnetic order along the *c* axis and 120° triangular order in the *c* plane. This configuration has been found for the most part of the *ABX*₃ antiferromagnets, with the interesting exception of RbMnBr₃ where an incommensurate helix configuration has been seen.^{17,18} We think that this surprising configuration could be explained only if further frustration mechanisms such as exchange competition between different shells of neighbors were accounted for. Here we limit ourselves to nearest neighbor interactions as from Hamiltonian (2.1). Moreover, we suppose that the presence of the magnetic field leaves the magnetic cell unchanged. This is confirmed experimentally since no shift of the Bragg peaks with field is seen.¹³

We look for the minimum energy spin configurations in a classical approximation, where the spins are represented by classical vectors

$$\mathbf{S} = S (\sin \theta_s \cos \phi_s, \sin \theta_s \sin \phi_s, \cos \theta_s). \quad (2.2)$$

In (2.2), $s = 1, 2, 3$ labels the three sublattices in a *c* plane, and $s = 4, 5, 6$ labels the same sublattices in an adjacent plane. θ_s, ϕ_s are the polar and azimuthal angles with respect to the *c* axis we assume to coincide with the *z* axis. Substitution of (2.2) in (2.1) leads to the reduced energy

$$\begin{aligned} e_0 = \frac{E_0}{2J_{\parallel}NS^2} = & \frac{1}{3} [\sin \theta_1 \sin \theta_4 \cos(\phi_1 - \phi_4) + \cos \theta_1 \cos \theta_4 \\ & + \sin \theta_2 \sin \theta_5 \cos(\phi_2 - \phi_5) + \cos \theta_2 \cos \theta_5 + \sin \theta_3 \sin \theta_6 \cos(\phi_3 - \phi_6) + \cos \theta_3 \cos \theta_6] \\ & + \frac{1}{2} j [\sin \theta_1 \sin \theta_2 \cos(\phi_1 - \phi_2) + \cos \theta_1 \cos \theta_2 + \sin \theta_2 \sin \theta_3 \cos(\phi_2 - \phi_3) + \cos \theta_2 \cos \theta_3 \\ & + \sin \theta_3 \sin \theta_1 \cos(\phi_3 - \phi_1) + \cos \theta_3 \cos \theta_1 + \sin \theta_4 \sin \theta_5 \cos(\phi_4 - \phi_5) + \cos \theta_4 \cos \theta_5 \\ & + \sin \theta_5 \sin \theta_6 \cos(\phi_5 - \phi_6) + \cos \theta_5 \cos \theta_6 + \sin \theta_6 \sin \theta_4 \cos(\phi_6 - \phi_4) + \cos \theta_6 \cos \theta_4] \\ & + \frac{1}{6} d (\cos^2 \theta_1 + \cos^2 \theta_2 + \cos^2 \theta_3 + \cos^2 \theta_4 + \cos^2 \theta_5 + \cos^2 \theta_6) \\ & - \frac{1}{3} h (\sin \theta_1 \cos \phi_1 + \sin \theta_2 \cos \phi_2 + \sin \theta_3 \cos \phi_3 + \sin \theta_4 \cos \phi_4 + \sin \theta_5 \cos \phi_5 + \sin \theta_6 \cos \phi_6), \quad (2.3) \end{aligned}$$

where E_0 is the classical energy of the model and $j = J_{\perp}/J_{\parallel}$, $d = D/2J_{\parallel}$, $h = g\mu_B H/4J_{\parallel}S$. In Eq. (2.3) the external magnetic field is assumed to be parallel to a row of in-plane nearest neighbors. In our choice of reference system this is the *x* axis. When the external magnetic field is directed along the *c* (*z*) axis the reduced energy is

still given by (2.3) where the contribution proportional to h has to be replaced by

$$-\frac{1}{3} h (\cos \theta_1 + \cos \theta_2 + \cos \theta_3 + \cos \theta_4 + \cos \theta_5 + \cos \theta_6). \quad (2.4)$$

Minimization of e_0 with respect to the 12 variables θ_s, ϕ_s , is performed numerically. We find that for small j the only stable configurations when the external magnetic field increases from zero to the saturation field are an in-plane phase (H/F) characterized by

$$\begin{aligned} \theta_s &= \frac{\pi}{2}, \quad s = 1, \dots, 6, \\ \phi_4 &= -\phi_1, \quad \phi_5 = -\phi_3, \quad \phi_6 = -\phi_2, \end{aligned} \quad (2.5)$$

where ϕ_1, ϕ_2, ϕ_3 are solutions of the equations

$$\begin{aligned} \sin(2\phi_1) + \frac{3}{2}j[\sin(\phi_1 - \phi_2) + \sin(\phi_1 - \phi_3)] - h \sin \phi_1 &= 0, \\ \sin(\phi_2 + \phi_3) + \frac{3}{2}j[\sin(\phi_2 - \phi_3) + \sin(\phi_2 - \phi_1)] - h \sin \phi_2 &= 0, \\ \sin(\phi_2 + \phi_3) + \frac{3}{2}j[\sin(\phi_3 - \phi_1) + \sin(\phi_3 - \phi_2)] - h \sin \phi_3 &= 0, \end{aligned} \quad (2.6)$$

and a U phase with the axis directed along the field (x axis) characterized by

$$\theta_4 = \theta_1 = \frac{\pi}{2}, \quad \theta_6 = \theta_2, \quad \theta_5 = \theta_3 = \pi - \theta_2, \quad \phi_4 = -\phi_1, \quad \phi_5 = \phi_6 = -\phi_2, \quad \phi_3 = \phi_2, \quad (2.7)$$

where ϕ_1, ϕ_2, θ_2 are solutions of the equations

$$\begin{aligned} \sin(2\phi_1) + 3j \sin \theta_2 \sin(\phi_1 - \phi_2) - h \sin \phi_1 &= 0, \\ \sin \theta_2 [\sin \theta_2 \sin(2\phi_2) + \frac{3}{2}j \sin(\phi_2 - \phi_1) - h \sin \phi_2] &= 0, \\ \cos \theta_2 \left\{ \sin \theta_2 [1 + \cos(2\phi_2)] + \frac{3}{2}j [\cos(\phi_1 - \phi_2) + 2 \sin \theta_2] - d \sin \theta_2 - h \cos \phi_2 \right\} &= 0. \end{aligned} \quad (2.8)$$

When the field is directed along the c (z) axis the stable configuration is a ‘‘cone’’ configuration with the axis along the field and apex angle

$$\theta = \cos^{-1} \frac{2h}{4 + 9j + 2d}. \quad (2.9)$$

The polar angles are given by $\phi_1 = \phi$, $\phi_2 = \phi + \frac{2\pi}{3}$, $\phi_3 = \phi - \frac{2\pi}{3}$, $\phi_4 = \phi + \pi$, $\phi_5 = \phi - \frac{\pi}{3}$, $\phi_6 = \phi + \frac{\pi}{3}$. The arbitrary ϕ angle reflects the invariance of Hamiltonian (2.1) under rotation about the z axis when the field is along the c axis.

The solutions of Eq. (2.6) correspond to a distorted helix for $h < h_0 \simeq \sqrt{3j}$ and to a fan ($\phi_2 = \phi_3$) for $h > h_0$. The H-F transition is continuous and independent of the anisotropy. These phases are the same as those found in a Heisenberg model with large single-ion easy-plane anisotropy² or in a planar model.¹⁹ At $h = h_s = 2 + \frac{9}{2}j$ a continuous transition to the saturated phase occurs. We find that the U phase occurs for small single-ion easy-plane anisotropy $d < d_0 \simeq 3j/2$ in agreement with a calculation at leading order in d and j .²⁰

The phase diagram in the j - d - h space is sketched in Fig. 1. For $j = 0$ (noninteracting antiferromagnetic linear chains) one has the usual spin-flop (SF) phase that goes continuously into the saturated (S) phase. For $j \neq 0$ any h - d plane is divided into four regions. For $d < d_0$ one finds H, U, F, and S phases at increasing magnetic field. The H-U transition is first order, while the U-F and F-S transitions are continuous. Indeed Eqs. (2.8) reduce to Eqs. (2.6) with $\phi_2 = \phi_3$ when $\theta_2 = \frac{\pi}{2}$, so that

the U phase changes continuously into the F phase. The H-U transition occurs at low field ($0 < h_1 < h_0$ where h_1 depends on the anisotropy strength), while the U-F transition occurs very close to the saturation field, so that the U phase is stable over a wide range of magnetic fields. The H-U and U-F boundary lines meet at a triple point (h_0, d_0) above which only the H, F, S phases exist.

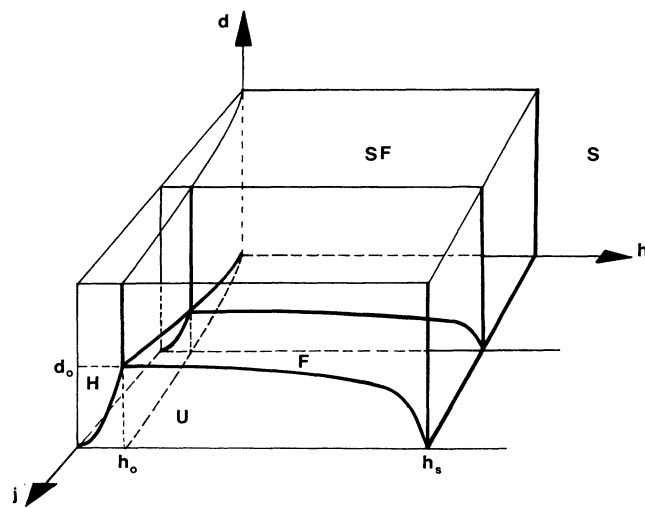


FIG. 1. Sketch of the phase diagram in the j - d - h space. H, U, F, SF, and S mean distorted helix, umbrella, fan, spin-flop, and saturated phases, respectively. $d_0 \simeq \frac{3}{2}j$, $h_0 \simeq (3j)^{\frac{1}{2}}$ is a line of triple points. $h_s = 2 + \frac{9}{2}j$ is the saturation field.

For $d = 0$ the U phase coincides with a cone phase with the axis along the x axis and apex angle $\theta = \cos^{-1}(\frac{2h}{4+9j})$ and it is stable over the whole range of magnetic fields ($0 < h < h_s$). For $j = 0.01$ we find that the U phase is stable for $0.079 < h < 2.040$, $0.144 < h < 2.013$, $0.157 < h < 1.985$, $0.170 < h < 1.859$, for $d = 0.003$, 0.010 , 0.012 , 0.014 , respectively. The triple point is at $d_0 = 0.015$, $h_0 = 0.176$. Note the flatness of the U-F transition line close to the triple point. One should also notice that in the U phase the spins 1,4 and 2,3,5,6 lie on the surface of two cones with the same axis but with different apex angles ϕ_1 , and $\cos^{-1}(\sin \theta_2 \cos \phi_2)$, respectively, where ϕ_1, ϕ_2, θ_2 are solutions of Eqs. (2.8). In the U phase the change of ϕ_1, ϕ_2, θ_2 with the field is very smooth: For small fields, say, $h < 0.5$, that is, for fields that can be obtained in the laboratory, one has $\phi_1 \simeq -\frac{\pi}{2} + \frac{1}{2}h$, $\phi_2 \simeq \frac{\pi}{2} - \frac{j-d/3}{j}h$, $\theta_2 = \sin^{-1}(\frac{j}{2j-2d/3})$. Figure 2 shows the H-F second-order phase transition giving the angles ϕ_1, ϕ_2, ϕ_3 as function of h for $d > d_0$.

We have evaluated analytically the anisotropy d_0 and the field h_0 corresponding to the triple point as a series expansion of j . Arriving at the triple point from the fan phase one can see from the numerical calculations that $\phi_1 \simeq -\pi/2$ and $\phi_2 = \phi_3 \simeq \pi/2$ so that we assume

$$\phi_1 = -\frac{\pi}{2} + \alpha \quad , \quad \phi_3 = \phi_2 = \frac{\pi}{2} - \beta \quad , \quad (2.10)$$

where α and β are small. In terms of these new variables Eqs. (2.6) read

$$\begin{aligned} 2 \sin \alpha \cos \alpha + 3j(\sin \alpha \cos \beta + \cos \alpha \sin \beta) \\ - h_0 \cos \alpha = 0 \quad , \end{aligned} \quad (2.11)$$

$$\begin{aligned} 2 \sin \beta \cos \beta + \frac{3}{2}j(\sin \alpha \cos \beta + \cos \alpha \sin \beta) \\ - h_0 \cos \beta = 0 \quad . \end{aligned}$$

Since the H-F transition is continuous, the Hessian of the reduced energy vanishes at $h = h_0$. This implies

$$\frac{3}{2}j(2 - \cos \alpha \cos \beta + \sin \alpha \sin \beta) - h_0 \sin \beta = 0 \quad . \quad (2.12)$$

Moreover, at the triple point the spins of the U configuration collapse into the c plane, so that the third equation of (2.8) leads to

$$\begin{aligned} 1 - \cos(2\beta) + \frac{3}{2}j(2 - \cos \alpha \cos \beta + \sin \alpha \sin \beta) \\ - h_0 \sin \beta - d_0 = 0 \quad . \end{aligned} \quad (2.13)$$

Solution of Eqs. (2.11), (2.12), (2.13) is

$$\begin{aligned} \sin \alpha &= \sqrt{1 - \cos^2 \beta \left(2 - \frac{4}{3j} \sin^2 \beta\right)^2} \quad , \\ \sin \beta &= \frac{1}{2} \sqrt{3j(1 + X)} \quad , \\ h_0 &= 2 \sin \beta \left(\frac{3}{2}j + \cos^2 \beta\right) \\ &\quad + \frac{3}{2}j \sqrt{1 - \cos^2 \beta \left(2 - \frac{4}{3j} \sin^2 \beta\right)^2} \quad , \\ d_0 &= 2 \sin^2 \beta \quad , \end{aligned} \quad (2.14)$$

where X is the solution of the equation

$$\begin{aligned} \left(\frac{9}{8}j^2 - \frac{3}{4}j\right) X^4 + \left(\frac{9}{16}j^2 - \frac{3}{4}j + 1\right) X^3 \\ - \left(\frac{9}{8}j^2 - \frac{3}{4}j + 2\right) X^2 + \left(\frac{9}{16}j^2 + \frac{3}{4}j + 1\right) X + \frac{9}{8}j^2 = 0 \quad . \end{aligned} \quad (2.15)$$

For small j one has

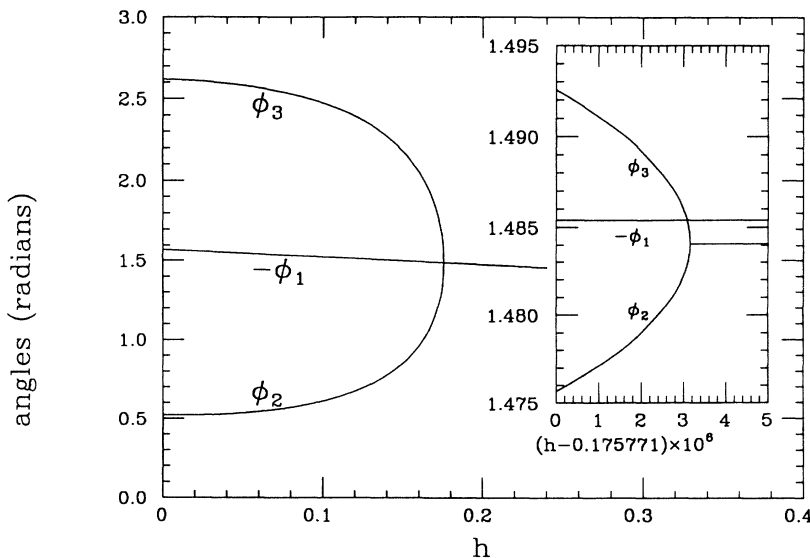


FIG. 2. Angles (in radians) of the planar (H/F) phase versus magnetic field for $j = 0.01$, $d > d_0 = 0.015$. Notice the H-F second-order phase transition at $h_0 = 0.17577315$ where $\phi_2 = \phi_3$. The inset shows that $\phi_1 \neq \phi_2$.

$$\sin \alpha = \frac{1}{2} \sqrt{3j} \left(1 - \frac{3}{2}j + \frac{9}{16}j^2 + \frac{189}{64}j^3 - \frac{1377}{64}j^4 + \dots \right), \quad (2.16)$$

$$\sin \beta = \frac{1}{2} \sqrt{3j} \left(1 - \frac{9}{16}j^2 + \frac{27}{64}j^3 + \frac{567}{512}j^4 - \frac{1701}{512}j^5 + \dots \right), \quad (2.17)$$

$$h_0 = \sqrt{3j} \left(1 + \frac{3}{2}j - \frac{27}{16}j^2 + \frac{81}{64}j^3 + \frac{1539}{512}j^4 - \frac{43011}{2048}j^5 + \dots \right), \quad (2.18)$$

$$d_0 = \frac{3}{2}j \left(1 - \frac{9}{8}j^2 + \frac{27}{32}j^3 + \frac{81}{32}j^4 - \frac{3645}{512}j^5 + \dots \right). \quad (2.19)$$

The first terms of h_0 and d_0 agree with those found in Ref. 20 where a leading order expansion was done.

III. NEUTRON-SCATTERING CROSS SECTION

The cross section for the coherent elastic magnetic scattering is²¹

$$\begin{aligned} \left(\frac{d\sigma}{d\Omega} \right)^{\text{el}} &= r_0^2 \left| \frac{1}{2} g F(\mathbf{k}) \exp\{-W(\mathbf{k})\} \right|^2 (NS)^2 \sum_{\mathbf{G}} \delta(\mathbf{k} - \mathbf{G}) \\ &\times \left\{ \left(1 - \frac{k_x^2}{k^2} \right) |m_x(\mathbf{G})|^2 + \left(1 - \frac{k_y^2}{k^2} \right) |m_y(\mathbf{G})|^2 + \left(1 - \frac{k_z^2}{k^2} \right) |m_z(\mathbf{G})|^2 \right\}, \end{aligned} \quad (3.1)$$

where

$$\begin{aligned} m_x(\mathbf{G}) &= \frac{1}{6} \sum_{s=1}^6 \exp\{i\mathbf{G} \cdot \boldsymbol{\delta}_s\} \sin \theta_s \cos \phi_s, \\ m_y(\mathbf{G}) &= \frac{1}{6} \sum_{s=1}^6 \exp\{i\mathbf{G} \cdot \boldsymbol{\delta}_s\} \sin \theta_s \sin \phi_s, \\ m_z(\mathbf{G}) &= \frac{1}{6} \sum_{s=1}^6 \exp\{i\mathbf{G} \cdot \boldsymbol{\delta}_s\} \cos \theta_s. \end{aligned} \quad (3.2)$$

The vectors $\boldsymbol{\delta}_1 = (0, 0, 0)$, $\boldsymbol{\delta}_2 = (a, 0, 0)$, $\boldsymbol{\delta}_3 = (2a, 0, 0)$, $\boldsymbol{\delta}_4 = (0, 0, c)$, $\boldsymbol{\delta}_5 = (a, 0, c)$, $\boldsymbol{\delta}_6 = (2a, 0, c)$ label the spins

of the unit magnetic cell. a is the nearest neighbor distance in the c plane and c is the nearest neighbor distance along the c axis:

$$\begin{aligned} \mathbf{G}(l', m', n') &= (l' + m') \frac{2\pi}{a} \hat{u}_x + (l' - m') \frac{2\pi}{\sqrt{3}a} \hat{u}_y \\ &+ n' \frac{2\pi}{c} \hat{u}_z, \end{aligned} \quad (3.3)$$

$$l' = \frac{2}{3}l - \frac{1}{3}m, \quad m' = -\frac{1}{3}l + \frac{2}{3}m, \quad n' = \frac{1}{2}n, \quad (3.4)$$

with l, m, n integers. In Table I we give the analytic forms

TABLE I. Magnetizations for the planar (P) (helix or fan) and umbrella (U) phases. In the P phase ϕ_1, ϕ_2, ϕ_3 are given by the solutions of Eqs. (2.6). In the U phase ϕ_1, ϕ_2, θ_2 are given by the solutions of Eqs. (2.8). The external magnetic field is applied along the x axis.

	P phase	U phase
$ m_x(0, 0, 0) $	$\frac{1}{3} \cos \phi_1 + \cos \phi_2 + \cos \phi_3 $	$\frac{1}{3} \cos \phi_1 + 2 \sin \theta_2 \cos \phi_2 $
$ m_y(0, 0, 0) $	0	0
$ m_z(0, 0, 0) $	0	0
$ m_x(\frac{1}{3}, \frac{1}{3}, \frac{1}{2}) $	$\frac{1}{2\sqrt{3}} \cos \phi_2 - \cos \phi_3 $	0
$ m_y(\frac{1}{3}, \frac{1}{3}, \frac{1}{2}) $	$\frac{1}{6} 2 \sin \phi_1 - \sin \phi_2 - \sin \phi_3 $	$\frac{1}{3} \sin \phi_1 - \sin \theta_2 \sin \phi_2 $
$ m_z(\frac{1}{3}, \frac{1}{3}, \frac{1}{2}) $	0	$\frac{1}{\sqrt{3}} \cos \theta_2$
$ m_x(\frac{1}{3}, \frac{1}{3}, 0) $	$\frac{1}{6} 2 \cos \phi_1 - \cos \phi_2 - \cos \phi_3 $	$\frac{1}{3} \cos \phi_1 - \sin \theta_2 \cos \phi_2 $
$ m_y(\frac{1}{3}, \frac{1}{3}, 0) $	$\frac{1}{2\sqrt{3}} \sin \phi_2 - \sin \phi_3 $	0
$ m_z(\frac{1}{3}, \frac{1}{3}, 0) $	0	0
$ m_x(0, 0, \frac{1}{2}) $	0	0
$ m_y(0, 0, \frac{1}{2}) $	$\frac{1}{3} \sin \phi_1 + \sin \phi_2 + \sin \phi_3 $	$\frac{1}{3} \sin \phi_1 + 2 \sin \theta_2 \sin \phi_2 $
$ m_z(0, 0, \frac{1}{2}) $	0	0

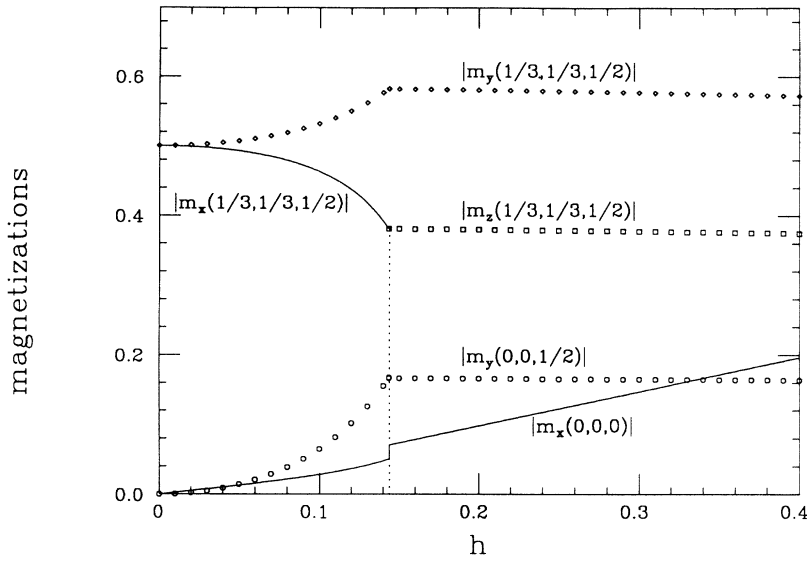


FIG. 3. Magnetizations $|m_\alpha(\mathbf{G})|$ as defined in Table I for $\mathbf{G} = (0, 0, 0)$ (uniform magnetization), $(\frac{1}{3}, \frac{1}{3}, \frac{1}{2})$ (staggered magnetization), and $(0, 0, \frac{1}{2})$, versus field for $j = 0.01$, $d = 0.01$. Notice the first-order H-U phase transition at $h = 0.144$.

of the magnetizations $|m_\alpha(\mathbf{G})|$ with $\alpha = x, y, z$, related to some Bragg peaks of interest for the planar and umbrella phase. Notice that $|m_x(0, 0, 0)|$ and $|m_x(\frac{1}{3}, \frac{1}{3}, \frac{1}{2})|$ are the components along the field of the uniform and staggered magnetization, respectively. The magnetizations of Table I are shown in Figs. 3 and 4 as function of the external field for $j = 0.01$ and $d = 0.01$. Notice the H-U transition at $h = 0.144$ singled out in Fig. 3 by a jump in the component along the field of the uniform

and staggered magnetization. The same quantities are given in Figs. 5 and 6 for $j = 0.01$ and $d > d_0 = 0.015$. Notice the continuous H-F transition at $h_0 = 0.176$.

Let us now list the intensity of some neutron scattering elastic peaks:

$$I(0, 0, 1) = I(1, -1, 0) = |m_x(0, 0, 0)|^2. \quad (3.5)$$

Notice that $I(1, 1, 0) = 0$ because of the factor in (3.1):

$$I\left(\frac{1}{3}, \frac{1}{3}, \frac{1}{2}\right) = \left(1 - \frac{k_x^2}{k^2}\right) \left|m_x\left(\frac{1}{3}, \frac{1}{3}, \frac{1}{2}\right)\right|^2 + \left|m_y\left(\frac{1}{3}, \frac{1}{3}, \frac{1}{2}\right)\right|^2 + \left(1 - \frac{k_z^2}{k^2}\right) \left|m_z\left(\frac{1}{3}, \frac{1}{3}, \frac{1}{2}\right)\right|^2, \quad (3.6)$$

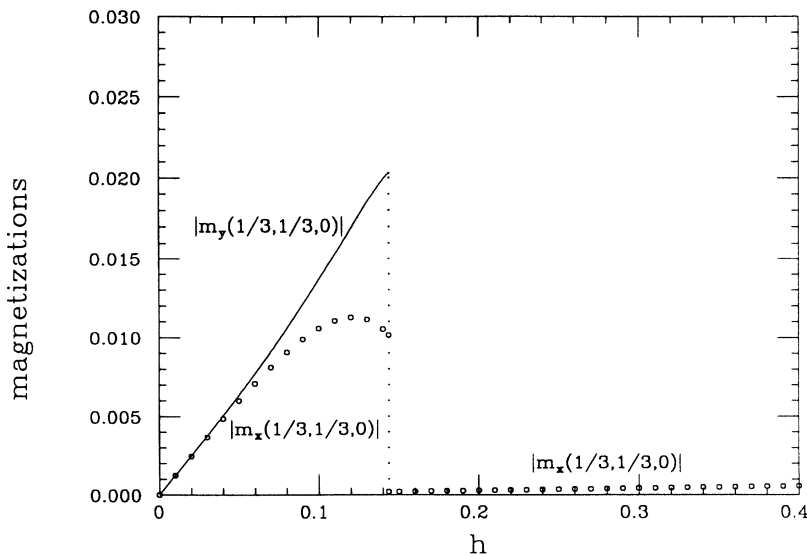


FIG. 4. The same as Fig. 3 but $\mathbf{G} = (\frac{1}{3}, \frac{1}{3}, 0)$.

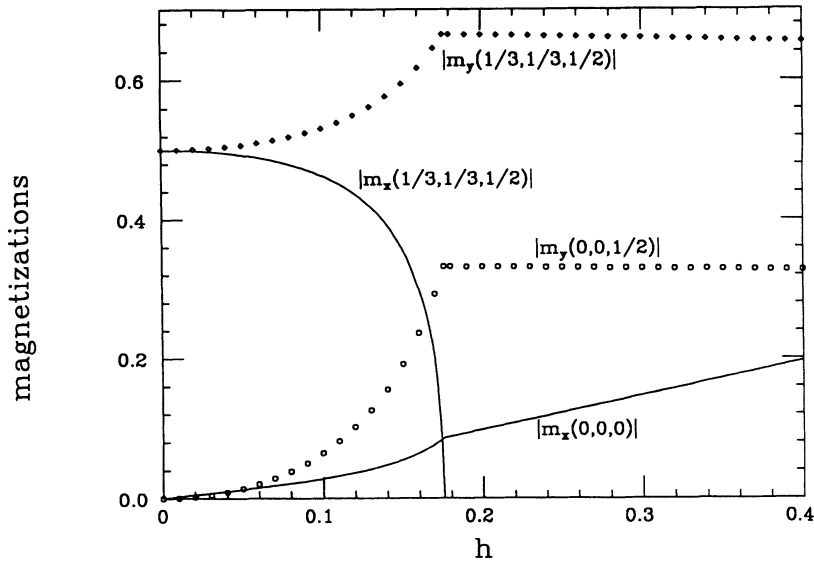


FIG. 5. The same as Fig. 3 but $d > d_0 = 0.015$. Notice the second-order H-F phase transition at $h_c = h_0 = 0.176$.

where $\mathbf{k} = (\frac{4\pi}{3a}, 0, \frac{\pi}{c})$,

$$I\left(\frac{1}{3}, \frac{1}{3}, 0\right) = \left| m_y\left(\frac{1}{3}, \frac{1}{3}, 0\right) \right|^2, \quad (3.7)$$

$$I\left(0, 0, \frac{1}{2}\right) = \left| m_y\left(0, 0, \frac{1}{2}\right) \right|^2. \quad (3.8)$$

Figure 7 gives some of the above quantities for CsMnBr_3 , for which we expect the high-anisotropy scenario because the parameters characterizing this compound¹³ are $j = 0.00216$ and $d = 0.00795$ greater than the triple-point anisotropy $d_0 = 0.00324$ obtained from Eq. (2.19). For this reason we expect a second-order H-F phase transition at $h_c = h_0 = 0.0808$ corresponding to $H_c = 6.2$ T as was suggested² and confirmed experimentally.¹³ No-

tice that the intensity of the $(0, 0, 1)$ peak shown in the inset of Fig. 7 has the right qualitative behavior as that observed experimentally (see inset of Fig. 1 of Ref. 13). Obviously our calculation refers to zero temperature so that no quantitative agreement on the transition field can be obtained with the experiment performed at $T = 7$ K. Anyway the kink related to the H-F transition is clearly seen in the inset of our Fig. 7. We expect an even more pronounced kink in the intensity of the $(\frac{1}{3}, \frac{1}{3}, \frac{1}{2})$ and $(0, 0, \frac{1}{2})$ peaks.

In Figs. 8, 9, and 10 we give the intensities of the $(\frac{1}{3}, \frac{1}{3}, \frac{1}{2})$, $(0, 0, \frac{1}{2})$, and $(0, 0, 1)$ peaks for CsVCl_3 , CsVBr_3 , and CsVI_3 , respectively. For these compounds we expect the occurrence of the U phase because the single-ion anisotropy is less than the triple-point anisotropy. Indeed the inelastic neutron scattering experiment¹⁵ suggests $j = 0.00006, 0.00025$, and

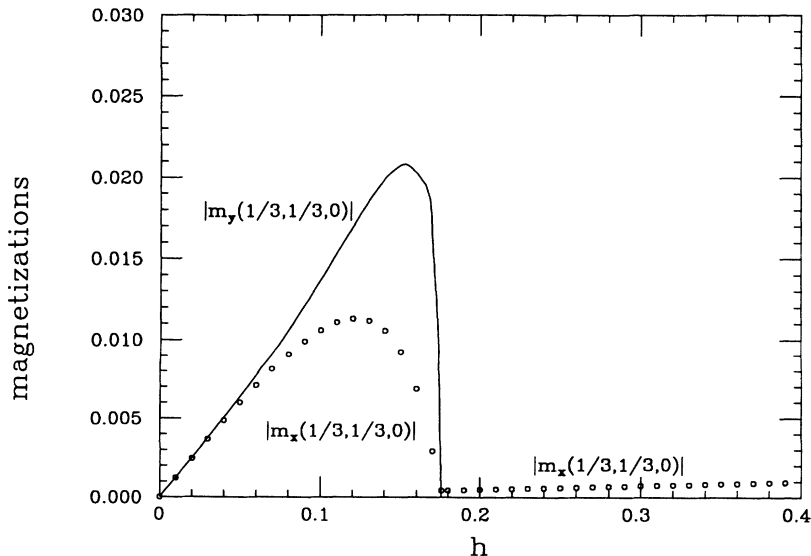


FIG. 6. The same as Fig. 5 but $\mathbf{G} = (\frac{1}{3}, \frac{1}{3}, 0)$.

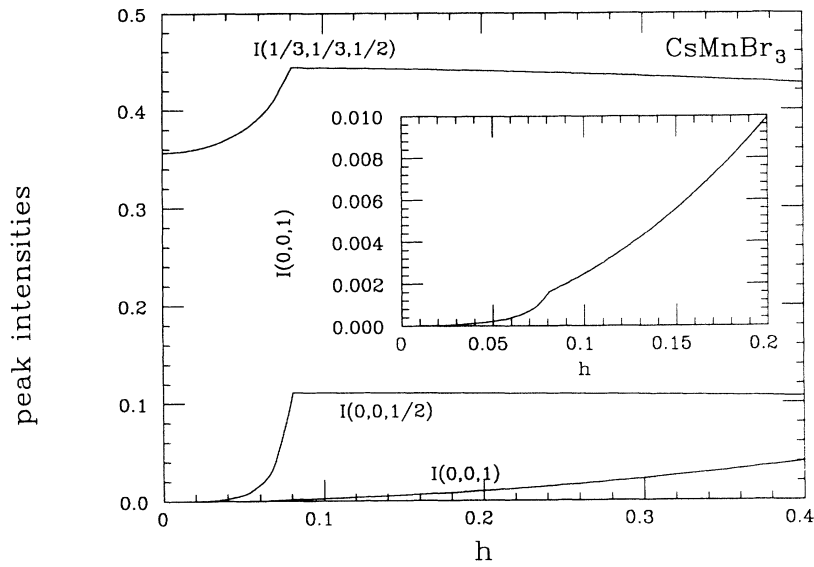


FIG. 7. Elastic-neutron-scattering peak intensity of CsMnBr_3 versus magnetic field ($j = 0.00216$, $d = 0.00795$). Notice the kink at the H-F continuous phase transition for $h_c = h_0 = 0.0808$ ($H_c = 6.2$ T).

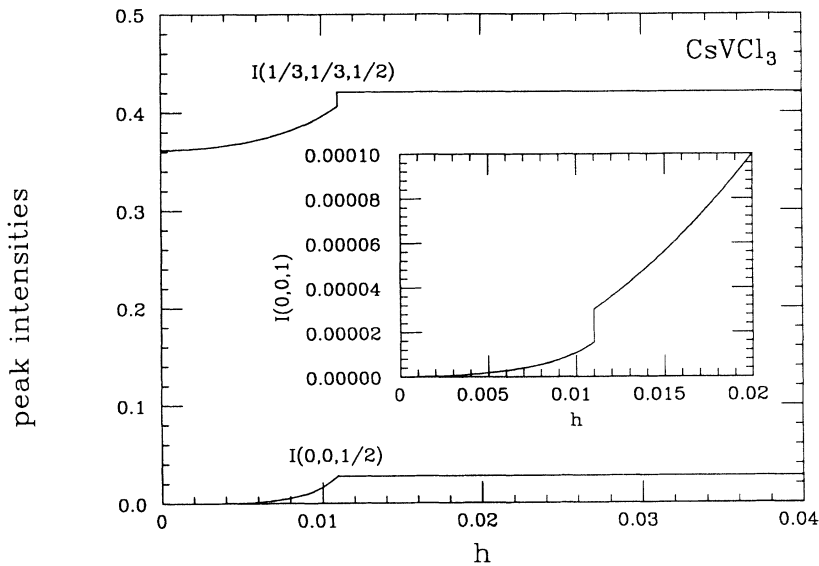


FIG. 8. Elastic-neutron-scattering peak intensity of CsVCl_3 versus magnetic field ($j = 0.00006$, $d = 0.00006$). Notice the jump at the H-U first-order phase transition for $h_1 = 0.0110$ ($H_1 = 5.7$ T).

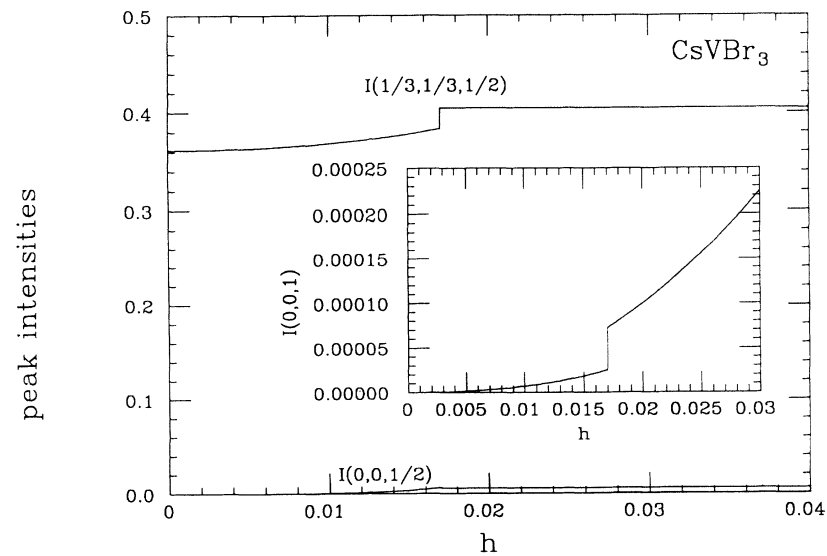


FIG. 9. Elastic-neutron-scattering peak intensity of CsVBr_3 versus magnetic field ($j = 0.00025$, $d = 0.00014$). Notice the jump at the H-U first-order phase transition for $h_1 = 0.0167$ ($H_1 = 6.2$ T).

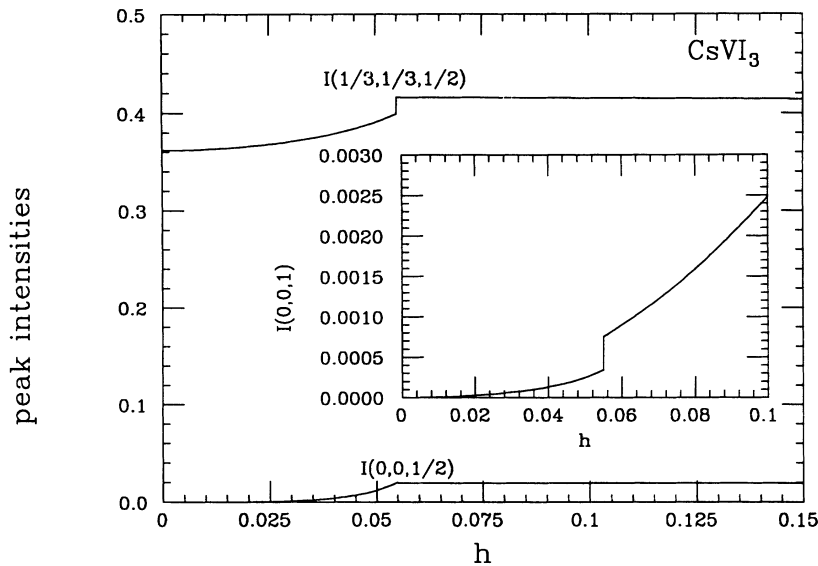


FIG. 10. Elastic-neutron-scattering peak intensity of CsVI_3 versus magnetic field ($j = 0.00168$, $d = 0.00149$). Notice the jump at the H-U first-order phase transition for $h_1 = 0.0547$ ($H_1 = 13.3$ T).

0.00168 and $d = 0.00006$, 0.00014, and 0.00149 for CsVCl_3 , CsVBr_3 , and CsVI_3 , respectively. The triple-point anisotropy is $d_0 = 0.00009$, 0.00038, and 0.00252, respectively, so that we expect the occurrence of the U phase for all three vanadium compounds. We have calculated the field at which the first-order H-U phase transition occurs and we have found $h_1 = 0.0110$, 0.0167, and 0.0547 corresponding to $H_1 = 5.7$, 6.2, and 13.3 T assuming $g = 2$, $S = 3/2$, and $J_{\parallel} = 10$, 7.1, and 4.7 meV, respectively.¹⁵ As one can see such fields can be easily obtained in the laboratory. In Figs. 8, 9, and 10 the H-U phase transition is revealed by a jump in the peak intensity so that the signature of this phase transition is easy to single out.

Elastic-neutron-scattering experiments on CsVCl_3 , CsVBr_3 , and CsVI_3 in an external magnetic field perpendicular to the c axis are suggested to test our theoretical expectation of the U phase.

IV. SUMMARY AND CONCLUDING REMARKS

The ABX_3 family, where A is an alkali element, B a magnetic ion, and X a halogen, can be modeled as for the magnetic properties by a hexagonal Heisenberg antiferromagnet with strong antiferromagnetic intrachain coupling and weak interchain coupling. In general a single-ion easy-plane anisotropy forces the spins in the c plane and the antiferromagnetic interchain coupling enters frustration owing to the triangular structure of the c plane. The elementary excitation spectrum is expected to show features related to the quantum antiferromagnetic chain¹² and peculiar reorientation phenomena should be induced by an external magnetic field.² This couple of reasons explains the high experimental interest for the ABX_3 compounds and the theoretical effort about models suitable to describe such compounds.

In this paper we have studied in a classical approximation the minimum energy spin configuration of a hexagonal Heisenberg antiferromagnet in an external magnetic

field perpendicular to the c axis for a generic single-ion easy-plane anisotropy (Sec. II). We have found that an *umbrella* phase occurs for intermediate magnetic fields, when the anisotropy is less than a critical value. The U phase intervenes between the low-field *distorted-helix* phase and the high-field *fan* phase. The H-U transition is first order; the U-F phase transition is second order as well as the F-S (saturated) phase transition. The U phase disappears above a triple point in the field-anisotropy plane where the only transitions are the second-order H-F and F-S ones. We stress that the U phase is stable over a substantial region in the parameter space. In Sec. III we have evaluated the elastic-neutron-scattering cross section for the different spin configurations. Application of our results to CsMnBr_3 agrees with previous expectation² of the second-order H-F phase transition. Indeed the easy-plane anisotropy of this compound is larger than the anisotropy characterizing the triple point. Moreover, the intensity of the $(0, 0, 1)$ peak we evaluated as function of the external magnetic field recovers the behavior observed experimentally.¹³

We expect that the U phase should occur in CsVCl_3 , CsVBr_3 , and CsVI_3 , where elastic- and inelastic-neutron-scattering experiments in zero field^{14,15} provide a set of Hamiltonian parameters which support such a phase. We expect that the signature of the H-U phase transition is a jump in the intensity of the elastic-neutron-scattering peak as a function of the external field as is shown in Figs. 8, 9, and 10. We suggest elastic-neutron-scattering experiments in an external magnetic field perpendicular to the c axis on the above mentioned vanadium compounds in order to test the existence of the umbrella spin configuration.

ACKNOWLEDGMENTS

This research was supported in part by INFN and CNR.

- ¹ N. Achiwa, J. Phys. Soc. Jpn. **27**, 561 (1969).
- ² A. V. Chubukov, J. Phys. C **21**, L441 (1988).
- ³ E. Rastelli and A. Tassi, Phys. Rev. B **49**, 9679 (1994).
- ⁴ A. V. Chubukov and D. I. Golosov, J. Phys. Condens. Matter **3**, 69 (1991).
- ⁵ E. Rastelli, A. Tassi, A. Pimpinelli, and S. Sedazzari, Phys. Rev. B **45**, 7936 (1992).
- ⁶ H. Kawamura, J. Phys. Soc. Jpn. **53**, 2452 (1984).
- ⁷ D. H. Lee, J. D. Joannopoulos, J. W. Negele, and D. P. Landau, Phys. Rev. Lett. **52**, 433 (1984); Phys. Rev. B **33**, 450 (1986).
- ⁸ W. Palme, F. Mertens, O. Born, B. Lüthi, and U. Schotte, Solid State Commun. **76**, 873 (1990).
- ⁹ A. E. Jacobs, T. Nikuni, and H. Shiba, J. Phys. Soc. Jpn. **62**, 4066 (1993).
- ¹⁰ H. Nojiri, Y. Tokunaga, and M. Motokawa, J. Phys. (Paris) Colloq. **49**, C8-1459 (1988).
- ¹¹ T. Nikuni and H. Shiba, J. Phys. Soc. Jpn. **62**, 3268 (1993).
- ¹² W. J. L. Buyers, R. M. Morra, R. L. Armstrong, M. J. Hogan, P. Gerlach, and K. Hirakawa, Phys. Rev. Lett. **56**, 371 (1986).
- ¹³ B. D. Gaulin, T. E. Mason, and M. F. Collins, Phys. Rev. Lett. **62**, 1380 (1989).
- ¹⁴ A. Hauser, U. Falk, P. Fischer, A. Furrer, and H. U. Güdel, J. Magn. Magn. Mater. **31-34**, 1139 (1983).
- ¹⁵ R. Feile, J. K. Kjems, A. Hauser, H. U. Güdel, U. Falk, and A. Furrer, Solid State Commun. **50**, 435 (1984).
- ¹⁶ H. Kadowaki, K. Ubukoshi, K. Hirakawa, D. P. Belanger, H. Yoshizawa, and G. Shirane, J. Phys. Soc. Jpn. **55**, 2846 (1986).
- ¹⁷ S. Kawano, Y. Ajiro, and T. Inami, J. Magn. Magn. Mater. **104-107**, 791 (1992).
- ¹⁸ L. Heller, M. F. Collins, Y. S. Yang, and B. Collier, Phys. Rev. B **49**, 1104 (1994).
- ¹⁹ M. L. Plumer and A. Caillé, Phys. Rev. B **42**, 10388 (1990).
- ²⁰ S. I. Abarzhi and A. V. Chubukov, J. Phys. Condens. Matter **2**, 9221 (1990).
- ²¹ S. W. Lovesey, *Theory of Neutron Scattering from Condensed Matter* (Clarendon Press, Oxford, 1984), Vol. 2, p. 256.